Ultrasonic study of the mixed-valence system $YbIn_{1-x}Ag_xCu_4$

S. Zherlitsyn,* B. Lüthi, and B. Wolf
Physikalisches Institut, Universität Frankfurt, Robert-Mayer Strasse 2-4, D-60054 Frankfurt, Germany

J. L. Sarrao
Los Alamos National Laboratory, Los Alamos, New Mexico 87545

Z. Fisk
National High Magnetic Field Laboratory and Florida State University, Tallahassee, Florida 32306

V. Zlatić
Institute of Physics, Zagreb, Croatia

(Received 12 February 1999)

We report ultrasonic investigation of the mixed-valence compounds $YbIn_{1-x}Ag_xCu_4$ for the different silver concentrations $x=0,\ 0.2,\ 0.25,\ 0.3$. This study enables us to characterize the coupling of the Yb ions with the lattice as a function of temperature, magnetic field, and silver concentration. For $x=0$ and 0.2 the system demonstrates pronounced first-order phase transition with the abrupt change in the different elastic moduli. For the higher silver concentrations we have observed rather smooth behavior of the elastic constants which is typical for a continuous phase transition. The critical temperature and the size of the anomaly in the bulk modulus at the phase transition changes linearly with silver concentration. External magnetic field shifts the transition to lower temperatures in accordance with previous investigations. Numerical calculations of the bulk modulus and the magnetic susceptibility have been performed in the frame of the promotional Ramirez-Falicov model. The results obtained demonstrate qualitative and quantitative agreement with the experimental data. [S0163-1829(99)06029-4]

I. INTRODUCTION

$YbInCu_4$ is the only stoichiometric compound which demonstrates first-order valence transition at ambient pressure.[1] Although the Yb valence reduction is rather small from 3 in the high temperature phase to 2.9 at low temperatures,[1,2] all physical parameters coupled to the *f*-electron occupation number n_f demonstrate anomalies in the vicinity of the phase transition.[1,3–7] The phase transition takes place at a critical temperature of $T_v \cong 40\,\mathrm{K}$, although some crystals showed the phase transition at temperatures up to 66 K.[3] Silver doping moves the transition to higher temperatures and makes it to be of second order.[6,8] Pure $YbAgCu_4$ appears to be a moderately heavy fermion ($\gamma = 250\,\mathrm{mJ/mol\,K^2}$) compound.[8,9] $YbInCu_4$ has a face-centered-cubic $C15b$ structure and the valence phase transition is accompanied by the abrupt increase in the lattice parameter by about 0.13% without any change in the space symmetry.[10,11] The cell volume was found to vary proportionally to n_f.[6] In addition to the change of the lattice parameter, the electrical resistivity shows an abrupt decrease at T_v. Hall coefficient measurement reveals a large change in carrier density, which occurs at the transition.[12] The magnetic susceptibility follows the Curie law at high temperatures with an effective magnetic moment that is close to the Yb^{3+} ($4f^{13}$, $J=7/2$) free-ion value $\mu = 4.54\mu_B$. The magnetic susceptibility drops suddenly at the phase transition and shows nearly temperature-independent Pauli-like paramagnetic behavior at low temperatures.[1,8] So far no magnetic order has been found in $YbInCu_4$ at low temperatures.[1] The Wilson ratio of the low-temperature susceptibility to the specific-heat constant γ (Ref. 13) and the temperature behavior of the Cu spin-lattice relaxation time, inferred from the nuclear quadrupole resonance (NQR) measurements[14] confirm a realization of the Fermi-liquid state below T_v. Effects of pressure and high magnetic field on the phase transition have been studied in a number of works.[2,15] It was shown that the field induced transition at $T<T_v$ is a valence transition with approximately the same change of valence as observed as a function of temperature at ambient field. It has been found that a simple energy scale with a rather small characteristic energy is associated with the phase transition,[15] and the silver doping does not change the scale relations. It turns out that the phase transition involves a large change of the Kondo temperature from $T_K \sim 20\,\mathrm{K}$ in the high-temperature phase to $T_K \sim 430\,\mathrm{K}$ at low temperatures.[8]

Earlier ultrasonic investigation[3,4] revealed a strong softening of the bulk modulus c_B of 43% at the transition temperature and a change of the Poisson ratio of 30%. At the same time transverse-acoustic modes demonstrated steplike anomalies in the sound velocity that was not typical for an isostructural phase transition. However, it is still unclear how the silver doping affects the coupling of the valence fluctuations to the lattice and how strong the stiffness of the lattice changes at the phase transition. In order to address this issue we have carried out the ultrasonic investigations of $YbIn_{1-x}Ag_xCu_4$ for different silver concentrations x in a wide temperature range and at applied external magnetic field. In addition we give a simple quantitative physical description of the temperature dependence of the elastic con-

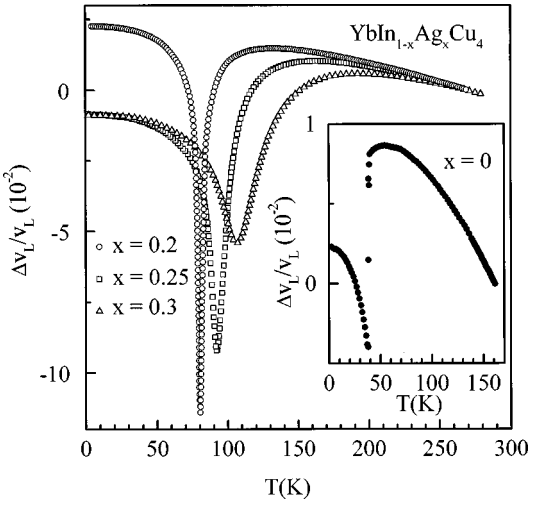

FIG. 1. Temperature behavior of the sound velocity of the longitudinal c_L mode ($\mathbf{k}\|\mathbf{u}\|[110]$; $\mathbf{k}$: wave vector, $\mathbf{u}$: polarization of the sound wave) in the vicinity of the mixed-valence transition in $YbIn_{1-x}Ag_xCu_4$ for the different silver concentrations x.

stants and magnetic susceptibility using a modified Ramirez-Falicov model.[17–21]

II. EXPERIMENTAL RESULTS

The samples were single crystals grown in $In_{1-x}Ag_xCu$ flux, as reported earlier.[8] The typical size of the samples used in our ultrasonic experiments was $1.2\times1.5\times1.5\,mm^3$. We utilized transverse resonant quartz transducers with a fundamental frequency of 10 MHz and piezoelectric films in case of longitudinal sound excitation. In order to reduce bond break effects at the discontinuous phase transition when the volume of the lattice increases by 0.5%, we used a thin In layer between the resonant transducers and the sample. Piezoelectric film was glued on the samples with a two component epoxy. Measurements were carried out at constant frequency. The ultrasonic pulse technique was described elsewhere.[22] Measurement at magnetic field up to 50 T was carried out using a pulse magnet with a typical magnetic pulse duration of 20 ms.

Figure 1 shows the temperature dependence of the sound velocity of the longitudinal $c_L=(c_{11}+c_{12}+2c_{44})/2$ mode in $YbIn_{1-x}Ag_xCu_4$ for different silver concentrations. In the case of pure $YbInCu_4$ there is a jump at the phase transition (see insert of Fig. 1). The ultrasonic signal becomes so small at the critical temperature $T_v\approx40\,K$ that it is impossible to measure the complete change of the sound velocity that takes place at the phase transition. Thus the inset of Fig. 1 shows a sound velocity behavior only in the immediate vicinity of the phase transition, but the real size of the anomaly and whether the sound velocity has a lower value in the low-temperature phase remains unknown. This behavior is typical for the discontinuous phase transition. Although the sound velocity of the c_L mode in $YbIn_{0.8}Ag_{0.2}Cu_4$ does not demonstrate a steplike behavior any more (see Fig. 1), the anomaly is very sharp and is located at higher temperatures ($T_v=80.2\,K$). Only after the first cooling the low-temperature shoulder of the anomaly is lower than the high-temperature shoulder (because of the discontinuous phase transition) but all following

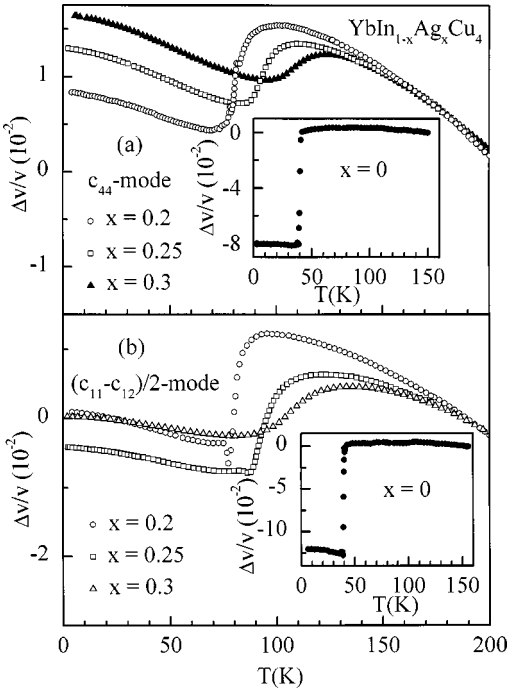

FIG. 2. Sound velocity of the transverse c_{44} mode ($\mathbf{k}\|[110]$, $\mathbf{u}\|[001]$) (a) and $(c_{11}-c_{12})/2$ mode ($\mathbf{k}\|[110]$, $\mathbf{u}\|[1\bar{1}0]$) (b) versus temperature at the mixed-valence phase transition in $YbIn_{1-x}Ag_xCu_4$ for the different silver concentrations x.

thermal cycles give the approximately symmetrical anomaly (shown in Fig. 1). The sound velocity of the c_L mode changes about 14% at the phase transition for this silver concentration. In both cases of silver concentration $x=0$ and $x=0.2$ we observed crystal degradation after a few cycles through the phase transition. As a result sound waves did not propagate through the degraded samples any more and one could see a mosaic structure, which appeared at a polished surface of the samples. This confirms the supposition about the first-order valence phase transition, taking place in $YbInCu_4$ and $YbIn_{0.8}Ag_{0.2}Cu_4$. Higher silver concentration moves the transition to higher temperatures and makes it continuous, consistent with Ref. 6. The critical temperature for $YbIn_{0.75}Ag_{0.25}Cu_4$ becomes $T_v=92\,K$ and for the highest concentration which we studied in this work, $YbIn_{0.7}Ag_{0.3}Cu_4$, the critical temperature is $T_v\approx106\,K$. In the last case the anomaly in the sound velocity is rather smooth but still the change of the sound velocity at the phase transition is more than 5%. One can see that both the critical temperature and size of anomaly changes approximately linearly with silver concentration. Figure 2 shows temperature dependencies of the sound velocity of the transverse c_{44} and $(c_{11}-c_{12})/2$ modes in the vicinity of the valence phase transition in $YbIn_{1-x}Ag_xCu_4$. Both transverse modes demonstrate identical steplike behavior. Anomalies in $YbInCu_4$ are very large $\Delta v/v\approx12\%$ for $(c_{11}-c_{12})/2$ mode and $\Delta v/v\approx8\%$ for c_{44} mode, (see insets of Fig. 2), although in $YbIn_{1-x}Ag_xCu_4$ ($x\neq0$) the change in the sound velocity is much smaller in comparison with c_L mode and transverse modes in pure $YbInCu_4$. The absolute sound velocity of different acoustic modes in cubic $YbIn_{1-x}Ag_xCu_4$ are listed in Table I.

TABLE I. Absolute sound velocities, critical temperature of the mixed-valence phase transition in $YbIn_{1-x}Ag_xCu_4$, and adjustable parameters in the Ramirez-Falicov model.

	Sound velocities at $T=170$ K							
x	c_L mode (km/s)	c_{44} mode (km/s)	$(c_{11}-c_{12})/2$ mode (km/s)	T_v (K)	E_f (meV)	G (meV)	W (meV)	b (meV)
0	4.28±0.1	2.49±0.1	2.04±0.1	40	18.4	53.8	1040	-
0.2	4.32±0.05	2.57±0.05	2.14±0.05	80.2	29	58	1040	100
0.25	4.33±0.05	2.54±0.05	2.13±0.05	92	29	55.5	1040	117
0.3	4.26±0.05	2.51±0.05	2.13±0.05	106	30.5	55	1080	200

At the isostructural valence transition in $YbInCu_4$ the bulk modulus $c_B=(c_{11}+2c_{12})/3$ should be soft.[3] We deduced the bulk modulus c_B from our experimental data (see Fig. 3, open symbols). One can see that for $YbIn_{0.75}Ag_{0.25}Cu_4$ and $YbIn_{0.7}Ag_{0.3}Cu_4$ the bulk modulus has a lower value in the mixed-valence phase in comparison with the high-temperature phase. It is impossible to ascertain this in case of $YbIn_{0.8}Ag_{0.2}Cu_4$ (and especially for $YbInCu_4$) because of some difficulties, mentioned above and associated with measurement of the sound velocity at the discontinuous phase transition with a large abrupt volume change. Qualitatively our results are consistent with the earlier ultrasonic investigation of $YbInCu_4$.[3] We have also deduced the Poisson ratio $\nu=c_{12}/(c_{11}+c_{12})$ (Fig. 4) and the elastic anisotropy factor $A=2c_{44}/(c_{11}-c_{12})$ (see inset of Fig. 4) from our experimental data. Both of these quantities show significant peculiarities at the valence phase transition, while ν decreases strongly at T_v for the different samples, it is still $\nu>0.2$. For simple cubic valence phase transition one could expect $\nu<0$.[23] Although the elastic anisotropy of $YbIn_{1-x}Ag_xCu_4$ is not very large (in fully isotropic case $A=1$), it changes at the phase transition, and the mixed-valence phase becomes slightly more anisotropic elastically (see inset of Fig. 4).

Applied magnetic field decreases the critical temperature of the valence phase transition.[15] We did not observe any shift of the critical temperature in $YbIn_{0.75}Ag_{0.25}Cu_4$ for **B** up to 13 T applied along [110] axis. Measurements performed in pulse magnetic field revealed a reduction of the critical temperature (see Fig. 5). This effect in the sound velocity of the longitudinal c_L mode turns out to be even larger than measured versus temperature at ambient pressure (see Fig. 1). The inset of Fig. 5 shows a part of the B-T phase diagram of $YbIn_{0.75}Ag_{0.25}Cu_4$ similar to the results obtained for other $YbIn_{1-x}Ag_xCu_4$ compounds.[15]

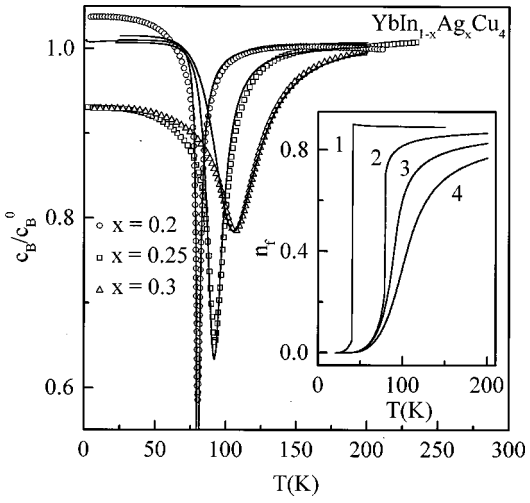

FIG. 3. Relative change of the bulk modulus $c_B=(c_{11}+2c_{12})/3$ (open symbols) as a function of temperature in the vicinity of the mixed-valence phase transition in $YbIn_{1-x}Ag_xCu_4$. Solid lines are results of numerical calculation in frame of the Ramirez-Falicov model (see text for details). Inset: results of numerical calculation of the *f*-level occupation probability versus temperature for $YbIn_{1-x}Ag_xCu_4$ in the frame of Ramirez-Falicov model [see Eq. (3)]. Values of the adjustable parameters are listed in Table I. Lines 1 to 4 correspond to different silver concentrations $x=0$, 0.2, 0.25, and 0.3.

III. DISCUSSION

Different theoretical approaches have been applied to explain the mechanism and driving forces for the valence transition. Of these the single impurity Anderson model which takes into account the hybridization of conduction electrons with localized *f* electrons cannot explain neutron-diffraction data[24] and photoemission spectra.[25] Likewise an extension to the Kondo-volume-collapse model (KVC),[26] which was considered for Ce $\alpha-\gamma$ phase transition, leads to unphysical

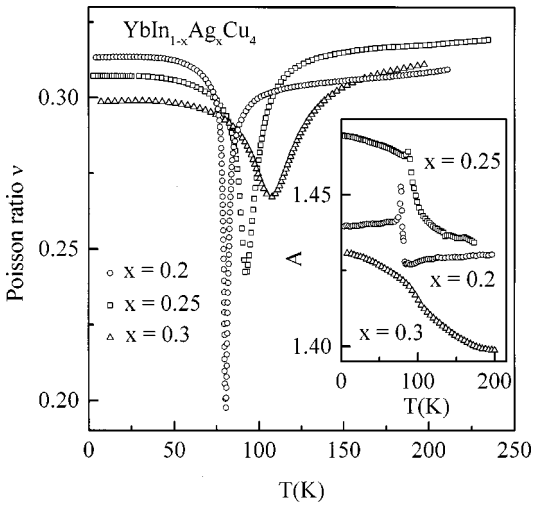

FIG. 4. Poisson ratio ν as a function of temperature in $YbIn_{1-x}Ag_xCu_4$ for the different silver concentrations x. The inset shows a change of the elastic anisotropy parameter $A=2c_{44}/(c_{11}-c_{12})$ at the mixed-valence phase transition in $YbIn_{1-x}Ag_xCu_4$. For an elastic isotropic crystal $A=1$.

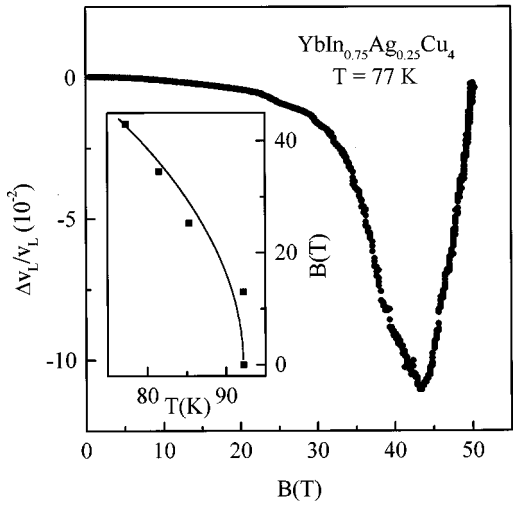

FIG. 5. Magnetic-field dependence of the sound velocity of the longitudinal c_L mode ($\mathbf{k}\|\mathbf{u}\|[110]$) at the metamagnetic mixed-valence transition in $YbIn_{0.75}Ag_{0.25}Cu_4$. Field sweep up is only shown. Magnetic field was applied along [001] direction. Temperature is 77 K. The inset shows a part of the B-T phase diagram, extracted from our pulse field ultrasonic measurements of $YbIn_{0.75}Ag_{0.25}Cu_4$ ($\mathbf{B}\|[001]$). Point at 13 T was extracted from temperature dependence of the sound velocity of the c_L mode at static magnetic field. In this case magnetic field was parallel to [110] crystallographic direction. The line was drawn to guide the eye.

large ($\Gamma \approx 4000$) electron Grüneisen parameter,[6] whereas this parameter was estimated to be only $\Gamma \approx 34$.[4]

Here we take the promotional Ramirez-Falicov model[17–21] to describe the thermodynamic properties of $YbIn_{1-x}Ag_xCu_4$ in the high-temperature phase (magnetic susceptibility, bulk elastic modulus). The observation of the crystal-field (CF) levels[16] and the Curie-Weiss law at high temperatures[1,8] points to a very small hybridization, which we neglect, so that the Ramirez-Falicov model can be used. The Ramirez-Falicov model was applied to the alpha-gamma transition in cerium, where the ground state consists of a filled Fermi sea and no f electrons. Localized single-particle excitations are obtained by promoting conduction electrons from the Fermi level to the localized energy level E_f above the chemical potential. As for the Yb ions, the f shell is fully occupied in the ground state, and the single-particle excitations are obtained by adding f holes rather than f electrons. If the conduction band has an electron-hole symmetry, the thermodynamic properties of Ce systems, with one f electron and Yb systems, with one f hole, are fully equivalent. To find the solution of the model for $T > T_v$ we use the mean-field approximation, following closely Refs. 17 and 18 where all the mathematical details can be found. For $T < T_v$, the hybridization effects will play an important role which we will not try to describe (see, for example Ref. 27). Likewise the question of the effect of fractional valence change of 3 to 2.9 we leave out from this analysis.[19] For $T < T_v$ an effective Hamiltonian, taking into account the hybridization, has to be used.

The free energy of the system can be written as the following:

$$F = E - TS, \tag{1}$$

where T is temperature, S is the entropy function, and E is an internal energy of given many-electron state, which in thermal equilibrium and for a fixed number of carriers can be written as[17]

$$E = E_{e,h} + NE_f n_f - NGn_f^2. \tag{2}$$

Here the first two terms represent single quasiparticle contributions of electrons and holes from the conduction band and highly localized f states, respectively. The last term is a quasiparticle-quasiparticle interaction, and $(-G)$ is an interaction constant between an electron in the f shell and a hole in a Wannier orbital. N is the number of Yb ions, n_f is the occupation probability of the f level, which has been found in Ref. 17:

$$n_f = \frac{12k_BT}{W} \ln\left|\frac{1 + A_0 e^{-Q_1}}{A_0 + e^{-Q_0}}\right|, \tag{3}$$

where

$$A_0 \equiv a \exp[(E_f - 2Gn_f)/k_BT], \tag{4}$$

$$a \equiv n_f/(2J+1)(1-n_f), \tag{5}$$

k_B is the Boltzmann constant, $W = W_e + W_h$ is the bandwidth of the conduction band, and W_e, W_h are electron and hole subbands, respectively, and

$$Q_0 \equiv W_h/k_BT, \quad Q_1 \equiv W_e/k_BT. \tag{6}$$

As discussed above in the case of Ce ions, an f count gives $n_f > 0$ for $T > T_v$ and $n_f = 0$ for $T < T_v$, where n_f is the concentration of f electrons. Similarly, for Yb ions, an f count also gives $n_f > 0$ for $T > T_v$ and $n_f = 0$ for $T < T_v$, but n_f is now the concentration of f holes. For Ce, we have to pay an energy $E_f > 0$, if we transfer an electron from the Fermi level in the conduction band to the localized f level above the chemical potential, i.e., Ce switches from the nonmagnetic $4f^0$ to the magnetic $4f^1$ configuration. In Yb case, we pay an energy $E_f > 0$, if we transfer an f electron from a localized level below the chemical potential to the Fermi level in the conduction band, i.e., if we produce an f hole such that the Yb ions switch from the nonmagnetic $4f^{14}$ to the magnetic $4f^{13}$ configuration. If the conduction band has electron-hole symmetry, the thermodynamic properties of Ce and Yb systems are exactly the same.

We assume a magnetoelastic expression for the coupling between f electrons and elastic waves:[28]

$$E_f = E_f^0 + b\varepsilon, \tag{7}$$

where E_f^0 is the position of the f level in the absence of volume deformation ε and b is a coupling constant. The entropy function in Eq. (1) is given by[17]

$$S = S_{e,h} - Nk_B[n_f \ln n_f + (1-n_f)\ln(1-n_f)] + Nk_B n_f \ln(2J+1). \tag{8}$$

The first term in Eq. (8) is the itinerant electron and hole entropy and the last two terms are the localized electron entropy and the ionic spin entropy, respectively. For our purposes we consider only the last two terms.

The bulk elastic modulus is written as a second derivative of the free energy:

$$c_B = \frac{\partial^2 F}{\partial \varepsilon^2} = \frac{\partial^2 E}{\partial \varepsilon^2} - T\frac{\partial^2 S}{\partial \varepsilon^2}. \tag{9}$$

Neglecting a conduction-band dependence on deformation and using Eqs. (1)–(9) we get an expression for the change of the bulk modulus as a function of temperature:

$$c_B - c_B^0 = N\frac{\partial n_f}{\partial \varepsilon}\left[2b - 2G\frac{\partial n_f}{\partial \varepsilon} + k_B T\frac{\partial n_f}{\partial \varepsilon}\left(\frac{1}{n_f} + \frac{1}{1-n_f}\right)\right], \tag{10}$$

where c_B^0 is the bare bulk modulus and

$$\frac{\partial n_f}{\partial \varepsilon} = 12b\left(\frac{W}{A_0[(\exp Q_1 + A_0)^{-1} - (\exp(-Q_0) + A_0)^{-1}]} - \frac{12k_B T}{n_f(1-n_f)} + 24G\right)^{-1}. \tag{11}$$

In Eq. (10) we neglected also the terms which contain a second derivative $\partial^2 n_f/\partial \varepsilon^2$. These Van Vleck terms contribute only marginally to c_B and they disappear automatically with approximations made in Ref. 18. The model is very sensitive to the values of the adjustable parameters, which are conduction bandwidth W, position of the f level E_f and coupling constants b and G. For a given temperature Eq. (3) yields three different solutions[17,18] and it is necessary to perform numerical calculations in order to get an absolute minimum of the free energy. Depending on the values of the parameters this model leads to the discontinuous or continuous phase transition at different temperatures. We have carried out numerical calculations and the inset of Fig. 3 shows the temperature behavior of the f-level occupation probabilities [see Eq. (3)]. This n_f for electrons is equivalent to the hole count because of electron-hole symmetry as discussed above. Figure 3 demonstrates a fit for a bulk elastic modulus change [see Eq. (10)] for the same adjustable parameters. These parameters are given in Table I. Within a slight variation of a few percent G, E_f, and W can give equally good fits of the bulk modulus but with quite different magnetoelastic coupling constant b. That is why b varies so strongly in Table I. A generalization of the Ramirez-Falicov model developed in Ref. 18 leads to qualitatively the same result. An approach made in Ref. 18 adds one additional contribution $NW(\partial n_f/\partial \varepsilon)^2/12$ to Eq. (10) and gives a value of the magnetoelastic coupling constant b to be about 2–4 times larger. b gives a bare electron Grüneisen parameter slightly smaller than the one deduced from $\partial T_c/\partial P$.[4] We would like to point out that the same parameters result in a qualitative and satisfactory quantitative description of the temperature dependence of the magnetic susceptibility (see Fig. 6) and the thermal expansion (see inset in Fig. 6) in the vicinity of the mixed-valence phase transition in $YbIn_{1-x}Ag_xCu_4$. Note that we can explain the volume change up to 0.2% instead of the measured total change of 0.5%.[6] The model leads to a change of the f-level occupation probability to be almost unity at the phase transition (see inset of Fig. 3) that is much more than observed in experiments. Some speculations about possible explanation of fractional valence change in

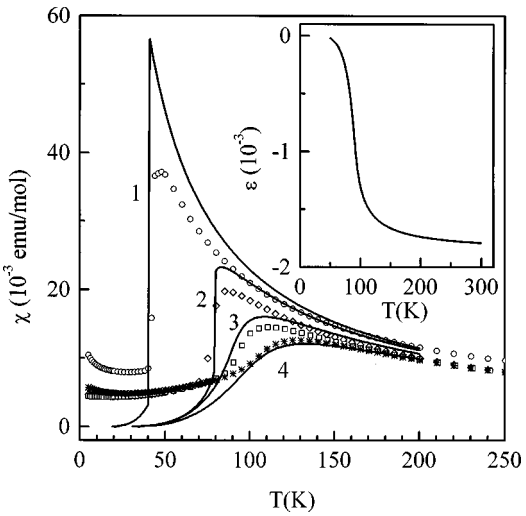

FIG. 6. Temperature dependence of the magnetic susceptibility $\chi = Ng^2 J(J+1)\mu_B^2 n_f/3k_B T$ (solid lines) calculated in the Ramirez-Falicov model with n_f shown in the inset of Fig. 3. Symbols are the experimental data taken from Ref. 8. Open circles correspond to $YbInCu_4$, diamonds to $x=0.2$, triangles to $x=0.25$, and stars to $x=0.3$ in $YbIn_{1-x}Ag_xCu_4$. The inset shows an equilibrium value of the volume deformation ε as a function of temperature, found as a result of free-energy minimization for the parameters corresponding to silver concentration $x=0.25$.

Ramirez-Falicov model are presented in Refs. 18 and 19, but both of them seem to be improper in the case of $YbIn_{1-x}Ag_xCu_4$. In order to account for the fractional valence change hybridization has to be taken into account. We leave also out of the consideration the theoretical description of the step function anomalies for the transverse sound near the mixed-valence phase transition which might be due to the strain-quadrupole coupling[28] as pointed out before.[4]

IV. CONCLUSIONS

In summary, we carried out the ultrasonic investigation of mixed-valence compounds $YbIn_{1-x}Ag_xCu_4$ for different silver concentration x. The obtained data confirm an important role of the lattice in the mixed-valence phase transition. For all investigated compounds large softening has been found for the bulk c_B modulus (see Fig. 3), longitudinal c_L modulus (see Fig. 1) and the Poisson ratio (see Fig. 4) at the phase transition. Transverse elastic moduli demonstrate much smaller steplike anomalies (see Fig. 2). The critical temperature and the size of the anomaly in the sound velocity of the c_L mode changes linearly with silver concentration. The anisotropy parameter A grows at the phase transition (see inset of Fig. 4), i.e., the mixed-valence state is slightly elastically more anisotropic than the high-temperature state. Applied magnetic field moves the valence transition towards lower temperatures in accordance with the earlier obtained results.[15] We used the promotional Ramirez-Falicov model in order to explain behavior of the bulk modulus and the magnetic susceptibility in the high-temperature phase. The properties of the model can be qualitatively understood by noticing that the increase of the internal energy due to the switching of some Yb ions from nonmagnetic $4f^{14}$ to the magnetic $4f^{13}$ configuration has to be compared with the

entropy gain due to the positional disorder and the spin disorder. At high enough temperatures, the entropy gain dominates over the energy loss in the free energy and all Yb ions switch to the magnetic configuration. The most important feature of the model is a driving by Coulomb repulsion between conduction and localized electrons phase transition which changes the *f* level occupation probability [see Eq. (3)]. A simple coupling mechanism with the elastic waves [see Eq. (7)] leads to the temperature dependence of the bulk modulus [see Eq. (10)]. Numerical calculations in the frame of this model show qualitative and quantitative agreement with the experimental data both for the bulk modulus and the magnetic susceptibility.

ACKNOWLEDGMENTS

This work was supported in part by the Deutsche Forschungsgemeinschaft under SFB 252 and the BMBF Project No. 13N6581A/3. Work at Los Alamos is performed under the auspices of the U.S. Department of Energy. The NHMFL is supported by the NSF and the state of Florida through Cooperative Agreement No. DMR-9527035. Z.F. and J.L.S. also acknowledge partial support from the NSF through Grant No. DMR-9501529. S.Z. would like to thank the members of the Physikalisches Institut der J. W. Goethe Universität for hospitality. V.Z. would like to thank the Alexander von Humboldt Foundation for support.

*On leave from Institute for Low Temperature Physics & Engineering, Kharkov, Ukraine.

[1] I. Felner and I. Nowik, Phys. Rev. B **33**, 617 (1986); I. Felner I. Nowik, D. Vaknin, Ulrike Potzel, J. Moser, G. M. Kalvius, G. Wortmann, G. Schmiester, G. Hilscher, E. Gratz, C. Schmitzer, N. Pollmayr, K. G. Prasad, H. de Waard, and H. Pinto, *ibid.* **35**, 6956 (1987); I. Nowik, I. Felner, J. Voiron, J. Beille, A. Najib, E. du Tremolet de Lacheisserie, and G. Gratz, *ibid.* **37**, 5633 (1988).

[2] J. M. De Tereza, Z. Arnold, A. del Moral, M. R. Ibarra, J. Kamarad, D. T. Adroja, and B. Rainford, Solid State Commun. **99**, 911 (1996).

[3] B. Kindler, D. Finsterbusch, R. Graf, F. Ritter, W. Assmus, and B. Lüthi, Phys. Rev. B **50**, 704 (1994).

[4] J. L. Sarrao, A. P. Ramirez, T. W. Darling, F. Freibert, A. Migliori, C. D. Immer, Z. Fisk, and Y. Uwatoko, Phys. Rev. B **58**, 409 (1998).

[5] M. Galli, F. Marabelli, and E. Bauer, Physica B **230-232**, 304 (1997).

[6] A. L. Cornelius, J. M. Lawrence, J. L. Sarrao, Z. Fisk, M. F. Hundley, G. H. Kwei, J. D. Thompson, C. H. Booth, and F. Bridges, Phys. Rev. B **56**, 7993 (1997).

[7] A. Continenza, P. Monachesi, M. Galli, F. Marabelli, and E. Bauer, Phys. Scr. **T66**, 177 (1997).

[8] J. L. Sarrao, C. D. Immer, C. L. Benton, Z. Fisk, J. M. Lawrence, D. Mandrus, and J. D. Thomoson, Phys. Rev. B **54**, 12 207 (1996).

[9] C. Rossel, K. N. Yang, M. B. Maple, Z. Fisk, E. Zirngiebl, and J. D. Thompson, Phys. Rev. B **35**, 1914 (1987).

[10] J. M. Lawrence, G. H. Kwei, J. L. Sarrao, Z. Fisk, D. Mandrus, and J. D. Thompson, Phys. Rev. B **54**, 6011 (1996).

[11] K. Kojima, Y. Nakai, T. Suzuki, H. Asano, F. Izumi, T. Fujita, and T. Hihara, J. Phys. Soc. Jpn. **59**, 792 (1990).

[12] E. Figueroa, J. M. Lawrence, J. L. Sarrao, Z. Fisk, M. F. Hundley, and J. D. Thompson, Solid State Commun. **106**, 347 (1998).

[13] K. Kojima, H. Hayashi, A. Minami, Y. Kasamatsu, and T. Hihara, J. Magn. Magn. Mater. **81**, 267 (1989).

[14] H. Nakamura, K. Nakajima, Y. Kataoka, K. Asayama, K. Yoshimura, and T. Nitta, J. Phys. Soc. Jpn. **59**, 28 (1990).

[15] C. D. Immer, J. L. Sarrao, Z. Fisk, A. Lacerda, C. Mielke, and J. D. Thompson, Phys. Rev. B **56**, 71 (1997).

[16] A. Severing, E. Gratz, B. D. Rainford, and K. Yoshimura, Physica B **163**, 409 (1990).

[17] R. Ramirez and L. M. Falicov, Phys. Rev. B **3**, 2425 (1971).

[18] M. Kiwi and R. Ramirez, Phys. Rev. B **6**, 3700 (1972).

[19] J. K. Freerics and V. Zlatic, Phys. Rev. B **58**, 322 (1998).

[20] L. M. Falicov and J. C. Kimball, Phys. Rev. Lett. **22**, 997 (1969).

[21] R. Ramirez, L. M. Falikov, and J. C. Kimball, Phys. Rev. B **2**, 3383 (1970).

[22] B. Lüthi, G. Bruls, P. Thalmeier, B. Wolf, D. Finsterbusch, and I. Kouroudis, J. Low Temp. Phys. **95**, 257 (1994).

[23] B. Lüthi, J. Magn. Magn. Mater. **52**, 70 (1985).

[24] J. M. Lawrence, R. Osborn, J. L. Sarrao, and Z. Fisk, Phys. Rev. B **59**, 1134 (1999).

[25] J. J. Joyce, A. J. Arko, J. L. Sarrao, K. Graham, and Z. Fisk, Philos. Mag. B **79**, 1 (1999).

[26] J. W. Allen and L. S. Liu, Phys. Rev. B **46**, 5047 (1992).

[27] M. Avignon and S. K. Ghatak, Solid State Commun. **16**, 1243 (1975).

[28] P. Thalmeier and B. Lüthi, in *Handbook on the Physics and Chemistry of Rare Earths*, edited by K. A. Gschneidner, Jr. and LeRoy Eyring (North-Holland, Amsterdam, 1991), Vol. 14.